Physics Letters B 816 (2021) 136192

Contents lists available at ScienceDirect

Physics Letters B

www.elsevier.com/locate/physletb

The short-range correlation of asymmetric *nucleonic* matter at finite temperature: The *LOCV* approach

Azar Tafrihi

Department of Physics, Isfahan University of Technology, Isfahan 84156-83111, Iran

ARTICLE INFO

Article history:
Received 5 January 2021
Received in revised form 1 March 2021
Accepted 1 March 2021
Available online 4 March 2021
Editor: J.-P. Blaizot

Keywords:
ASM
LOCV
Density distributions
Distribution functions
Quasideuteron
Bethe-Levinger factor

ABSTRACT

The short-range correlation of the asymmetric *nucleonic* matter (*ASM*) is perused at finite temperature in the lowest order constrained variational (*LOCV*) method. It is observed that, by increasing the temperature, the *LOCV ASM* static non-central distribution functions become weak. For small inter-particle distances, a universal behavior is found for the *LOCV ASM* state-dependent density distributions. Using the expectation value of the one-*pion* exchange part of the $AV18$ interaction, the scaling factor of the *pion* absorption cross section (the number of *quasideuterons*), for the different proton to neutron ratios R, is also estimated in the *LOCV* formalism. It is shown that, by increasing (decreasing) the ratio R (the temperature), the number of *quasideuterons* grows. Considering the scaling factor, the *Bethe-Levinger* (BL) factor for the *ASM* is also investigated. It is demonstrated that, at the saturation density and temperature 20 MeV, the BL factor for the *ASM* with $R = 1(0.5)$ becomes 4.3 (4.5).

1. Introduction

The study of the short-range structure of nuclei is an important topic in nuclear physics. The nuclei structure at the short inter-particle distances (high values of momentum) can be investigated, using the two-body state-dependent density (one-body momentum) distributions. At these mentioned limits, the nuclei density and momentum distributions show a universal behavior. The universality results from the short-range central and tensor correlations. Therefore, the nuclei state-dependent density distributions differ only by the scaling factor R_{Ad} at short distances [1]. The R_{Ad} factor, which represents the number of *quasideuterons*, is determined in terms of the *Bethe-Levinger* (BL) factor [1,2]. At high momentum transfer values, the cross sections of the scattering of photons, nucleons, and leptons off nuclei are also scaled. The scaling factors are proportional to the probability of the nuclei short-range two- and three-body correlations. Previously, the short-range structures of light nuclei and symmetric nuclear (pure neutron) matter were studied using the (Green's Function) Monte Carlo ($(GF)MC$), the Fermi *Hypernetted* chain (*FHNC*) and the Correlated Gaussian Basis (*CGB*) approaches, respectively [1–6]. The nuclei photo-disintegration cross section was also investigated by analyzing the corresponding experimental data and the *quasideuteron* model [7–9]. The scaling of the inclusive electron scattering cross sections of different nuclei and the probability of short-range two- and three-body correlations were also discussed in the references [10,11]. The thermal and *isospin* asymmetry effects on the behavior of nuclei one-body momentum distribution above the Fermi momentum were reported in the references [12,13]. Moreover, the scaling (and the BL) factor(s) for the momentum distributions of the symmetric nuclear matter and the heavy nuclei were evaluated, using the (correlated basis function approach [14,15]) convolution model [16]. The short-range structure and the scaling (BL) factor for the asymmetric *nucleonic* matter (*ASM*) at finite temperature, have not been reported yet.

Due to the importance of the microscopic study of the nuclei structure; in this research, the state-(in)dependent density distributions (distribution functions) and the estimations of the BL (scaling) factor for the *ASM* at finite temperature are found in the Lowest Order Constrained Variational (*LOCV*) formalism. In the present study, we employ the two-body $AV18$ [17] potential and the three-body interaction of the references [18,19]. In the *LOCV* calculations, the cluster expansion of the energy is truncated at the lowest order, i.e. at the two-body cluster term [20,21]. This approximation is justified by imposing the normalization constraint [22]. The *LOCV* framework was previously applied to different *nucleonic matter* problems at zero and finite temperatures [23–43]. The approximated *LOCV* predictions were in agreement with those of sophisticated *FHNC*, *MC* and *Brueckner-Hartree-Fock* (*BHF*) [5,44–52].

So, the outline of the present paper is as follows: (i) In section 2, the *LOCV* asymmetric *nucleonic* matter formalism at finite temperature and the corresponding state-(in)dependent density

E-mail address: tafrihi@iut.ac.ir.

https://doi.org/10.1016/j.physletb.2021.136192

distributions (distribution functions) formulas are given. (ii) In section 3, the *LOCV* asymmetric *nucleonic* matter data for zero, 10 and 20 MeV at 0.16 and 0.24 fm^{-3} are shown versus those of *MC*, *BHF* and *FHNC*. The *LOCV* estimations of the number of *quasideuterons* are also presented in the mentioned section.

2. The *LOCV* formalism at finite temperature

At finite temperature $\mathcal{T}$, the *ASM* Helmholtz free energy F per nucleon is obtained as follows [28]:

$$F = E - S\mathcal{T}, \tag{1}$$

where the *ASM* energy E per nucleon at the two-body cluster approximation and the entropy S per nucleon are respectively written as [28]:

$$E = E_1 + E_2 = \sum_{i=P,N} \frac{\hbar^2}{2m_i\pi^2\rho_i} \int dk n_i(k) k^4 + \frac{1}{2A}\sum_{ij}^{A} < ij|v_{eff}(12)|ij >_a, \tag{2}$$

$$S = -\frac{K}{A}\sum_{k,i=P,N} \{(1-n_i(k))\ln(1-n_i(k)) + n_i(k)\ln(n_i(k))\}, \tag{3}$$

where a means that the two-body state $|ij>$ is normalized and anti-symmetric, P (N) refers to the protons (neutrons), $m_{P(N)}$ is the mass of a proton (neutron) and A is the number of nucleons. Also, $\rho_{P,N}$ is the density of protons (neutrons) and k (K) is the momentum of a nucleon (the Boltzmann constant). The Fermi-Dirac distribution function for protons (neutrons) $n_{P(N)}(k)$ and the effective interaction $v_{eff}(12)$ are respectively given by [21,28]:

$$n_{P(N)}(k) = \{1 + exp[\beta(\epsilon_k^{P(N)} - \mu_{P(N)})]\}^{-1}, \tag{4}$$

$$v_{eff}(12) = -\frac{\hbar^2}{2m}[f(12), [\nabla_{12}^2, f(12)]] + f^{\dagger}(12)v(12)f(12), \tag{5}$$

with $\beta = (K\mathcal{T})^{-1}$, $\mu_{P(N)}$, m and $v(12)$ being the protons (neutrons) chemical potential, the average mass of nucleons and the two-body potential $AV18$ [17] with the three-body interaction of the reference [19], respectively. Note that, in our calculations, $K = 1$ and $\mathcal{T}$ is given in MeV. The protons (neutrons) single-particle energy $\epsilon_k^{P(N)}$ has the following form [28]:

$$\epsilon_k^{P(N)} = \frac{\hbar^2 k^2}{2m^*_{P(N)}}, \tag{6}$$

and the protons (neutrons) effective mass $m^*_{P(N)}$ is treated as a variational parameter [28]. The two-body correlation function $f(12)$ is also defined in terms of the correlations $f_{JSTT_z}(12)$ in the nucleon-nucleon state $JSTT_z$ (total angular momentum J, spin S, isospin T, isospin projection T_z), i.e. [39]:

$$f(12) = \sum_{JSTT_z} |JSTT_z > f_{JSTT_z}(12) < JSTT_z|, \tag{7}$$

where in the decoupled (coupled) states, the central (the central as well as the tensor-dependent) correlation functions are included [39]. The *LOCV ASM* correlation functions $f_{JSTT_z}(12)$ are obtained by minimization of the free energy F with respect to the normalization constraint, i.e. [22]:

$$\xi \equiv \rho \int d^3r_{12}(1 - g(r_{12})) - 1 = 0, \tag{8}$$

$$= \rho \int d^3r_{12}\{\sum_{\alpha \equiv JLSTT_zT_{z_1}T_{z_2}} \mathcal{C}_\alpha[(f^{\mathcal{T}}_{p,T_z}(r_{12}))^2 - f^2_{JSTT_z}(r_{12})]I^{\mathcal{T}}_{L,T_z}(r_{12})\} - 1 = 0, \tag{9}$$

and variation of $m^*_{P(N)}$ [31]. Note that the *ASM* density $\rho = \rho_P + \rho_N$ and the long-range part of $f_{JSTT_z}(r_{12})$, i.e. the *Pauli* functions $f^{\mathcal{T}}_{p,T_z}(r_{12})$, $\mathcal{C}_\alpha$ and $I^{\mathcal{T}}_{L,T_z}(r_{12})$ are given in the references [26,28,29,39]. Considering the above constraint, we arrive at a series of Euler-Lagrange differential equations [26,29,34]. For a given density, temperature and proton to neutron ratio, the *LOCV ASM* free energy F, energy E and entropy S are computed with the solutions of the mentioned Euler-Lagrange differential equations. Moreover, we can find the *LOCV ASM* operator-dependent nucleon-nucleon distribution functions (*NNDF*) at finite temperature as follows [39]:

$$g_p(r_{12}) = \sum_\alpha \mathcal{C}_\alpha (f^{\dagger}(12)O_p(12)f(12))_{JLSTT_z} I^{\mathcal{T}}_{L,T_z}(r_{12}), \tag{10}$$

where $O_{p=c,s,t,st,T,Tt,b,bt}(12)$ are the first eight operators of the $AV18$ interaction [17]. Multiplying $g_p(r_{12})$ by density ρ, we obtain the corresponding operator-dependent density distributions ρ_p. Using ρ_p, the state-dependent density distributions $\rho_{TSS_z}(\mathbf{r}_{12})$ (S_z is the spin projection) become [2,39]:

$$\rho_{100}(\mathbf{r}_{12}) = \frac{1}{16}\{3\rho_c(r_{12}) + \rho_t(r_{12}) - 3\rho_s(r_{12}) - \rho_{st}(r_{12})\}, \tag{11}$$

$$\rho_{000}(\mathbf{r}_{12}) = \frac{1}{16}\{\rho_c(r_{12}) - \rho_t(r_{12}) - \rho_s(r_{12}) + \rho_{st}(r_{12})\}, \tag{12}$$

$$\rho_{T10}(\mathbf{r}_{12}) = C_0(r_{12}) - 2C_2(r_{12})P_2(\cos\theta), \tag{13}$$

$$\rho_{T1\pm1}(\mathbf{r}_{12}) = C_0(r_{12}) + C_2(r_{12})P_2(\cos\theta), \tag{14}$$

where for $T = 0$ [2,39],

$$C_0(r_{12}) = \frac{1}{48}\{3\rho_c(r_{12}) - 3\rho_t(r_{12}) + \rho_s(r_{12}) - \rho_{st}(r_{12})\}, \tag{15}$$

$$C_2(r_{12}) = \frac{1}{48}\{\rho_T(r_{12}) - \rho_{Tt}(r_{12})\}, \tag{16}$$

and for $T = 1$ [2,39],

$$C_0(r_{12}) = \frac{1}{48}\{9\rho_c(r_{12}) + 3\rho_t(r_{12}) + 3\rho_s(r_{12}) + \rho_{st}(r_{12})\}, \tag{17}$$

$$C_2(r_{12}) = \frac{1}{48}\{3\rho_T(r_{12}) + \rho_{Tt}(r_{12})\}. \tag{18}$$

Note that $P_2(\cos\theta) = \frac{1}{2}(3\cos^2\theta - 1)$ and θ is the polar angle of $\mathbf{r}_{12}$ with respect to the spin-quantization axis $\hat{z}$ [1,39]. In section 3, using the expressions (1) to (3) and (10) to (14), we present the corresponding *LOCV ASM* data at finite temperature $\mathcal{T}$.

3. Results, discussions and conclusions

In this section, the *LOCV ASM* equation of state, the nucleon-nucleon distribution functions (*NNDF*), the state-dependent density distributions, the scaling and the *Bethe-Levinger* factors at zero and finite temperatures ($\mathcal{T}$) 10 and 20 MeV, using the $AV18$ potential [17] and the *TBI* of the reference [19], are investigated.

The *LOCV ASM* free energies for $R = 0(PNM), 0.5, 1(SNM)$ at $\mathcal{T}$=10, 20 MeV are plotted versus the *BHF* [53] and the Variational Chain Summation (*VCS*) results [5] for $R = 1$ in the Fig. 1. In the *BHF* and *VCS*, the $AV18$ with an effective *TBI* [54] and the $AV18 + Urbana\ IX$ *TBI* [55] were employed, respectively. The *LOCV SNM* free energies at $\mathcal{T}$=10 MeV lie near those of *BHF* and *VCS*. For

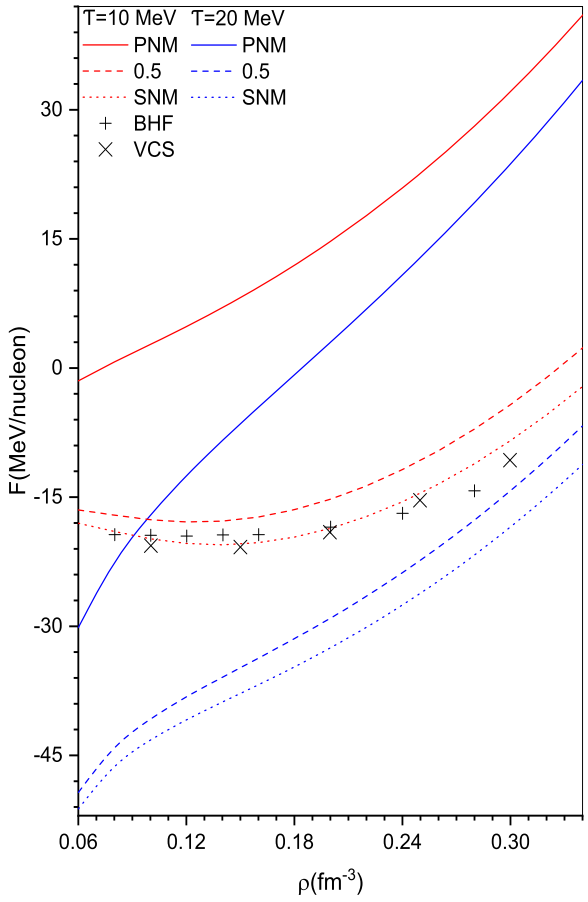

Fig. 1. (a) The *LOCV ASM* free energies at temperatures $\mathcal{T}$=10, 20 MeV, using the $AV18$ potential [17] and the *TBI* [19], for $R = 0(PNM), 0.5, 1(SNM)$. The corresponding *SNM VCS* (*VCS*) [5] and *BHF* (*BHF*) [53] calculations at $\mathcal{T}$=10 MeV are also shown for comparison.

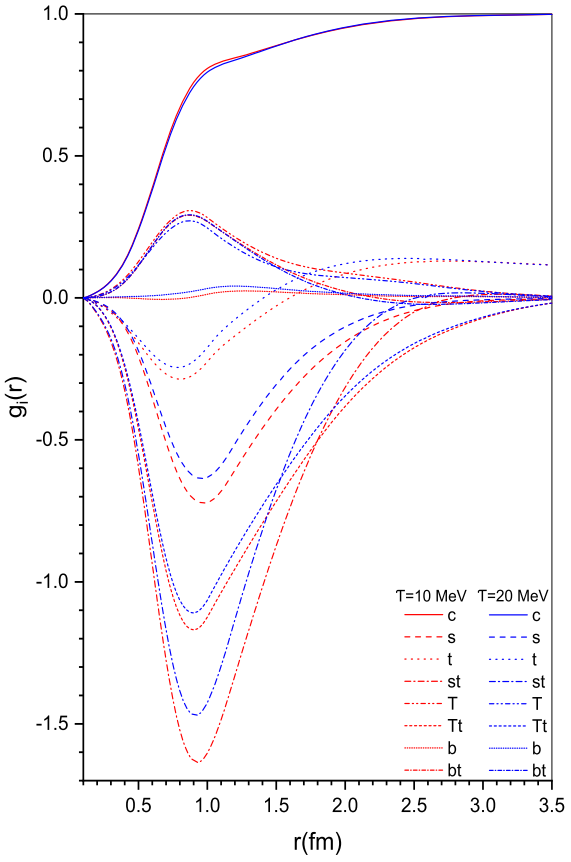

Fig. 2. The *LOCV ASM* central (c), spin- (s), *isospin*- (t), spin-*isospin*- (st), tensor- (T), tensor-*isospin*- (Tt), spin-orbit- (b) and spin-orbit-*isospin*-dependent (bt) nucleon-nucleon distribution functions for $\mathcal{T}$=10, 20 MeV and $R = 0.5$. The mentioned results are obtained at $\rho = 0.16$ fm^{-3}, using the $AV18$ potential [17] and the *TBI* [19].

a given density, by increasing the temperature (ratio R), the *ASM* free energies decrease.

In the Fig. 2, the *LOCV ASM* operator-dependent *NNDF* are plotted at $\mathcal{T}$=10,20 MeV, for $\rho = 0.16$ fm^{-3} and $R = 0.5$. Referring to the Fig. 2, one can see that the non-central *NNDF* are sensitive to the temperature changes more than those of central. At large inter-particle distances, the (non-)central *NNDF* tends to 1 (zero except that of *isospin*-dependent one). The non-central *NNDF* are big enough to confirm that the short-range correlations dominantly depend on the nucleon-nucleon (NN) spin and *isospin* [2]. The *NNDF* at $\mathcal{T}$=20 MeV lies above that of $\mathcal{T}$=10 MeV, except for the central and the tensor-dependent parts. This means that nucleons prefer to become tensor (spin-orbit) correlated at lower (higher) temperatures. The present *LOCV SNM* data differ from the corresponding *VCS* predictions of the reference [5], for which the two-body $AV18$, the three-body *Urbana IX* and the leading order relativistic boost interactions were included [5].

To have a better sense about the nucleon-nucleon (NN) correlations, one can study the NN density distributions in different TSS_z states. So, the *LOCV ASM* NN density distributions in the $TSS_z = 100,010$ states, at $\mathcal{T}$=10,20 MeV for $\rho = 0.16$ (0.24) fm^{-3}, are displayed in the panels (a) to (b) ((c) to (d)) of the Fig. 3. The ^2H (virtual bound state $^1S_0$ (*VBS*)) and the *SNM* NN density distributions of the reference [2] (AP) are also shown in the mentioned figure for comparison. In the panels (a) to (b) of the Fig. 3, the *LOCV ASM* $\rho_{100}(\mathbf{r})$ and the corresponding *VBS* and *SNM* data of the reference [2], are scaled to match the maximum value of the *LOCV PNM* $\rho_{100}(\mathbf{r})$ for $\mathcal{T}$=10 MeV. Similarly, in the panels (c) to (d) of the Fig. 3, the *LOCV ASM* $\rho_{010}(\mathbf{r})$ and the corresponding ^2H and *SNM* data of the reference [2], are scaled to match the maximum value of the *LOCV SNM* $\rho_{010}(\mathbf{r})$ at $\mathcal{T}$=10 MeV. Regarding the relations (11) to (12) ((13) to (14)), the $S = 0$ ($S = 1$) NN density distributions are isotropic (anisotropic). As it is demonstrated in the Fig. 3, $\rho_{100(010)}(\mathbf{r})$ are symmetric (show a quadrupole deformation). The maximum points of the *LOCV ASM* $\rho_{100}(\mathbf{r})$ are located at $r = 1fm$, where the nuclear force is most attractive. The short-range behavior of the scaled *SNM*, ^2H and *VBS* state-dependent density distributions of the reference [2] is consistent with that of *LOCV ASM*. As it is obvious in the panels (a) to (d) of the Fig. 3, at small inter-particle distances $r < 1fm$, the shape of the *LOCV* $\rho_{100,010}(\mathbf{r})$ is universal. So, one concludes that, at finite temperature, the universality of the *ASM* state-dependent NN density distributions behavior is valid for $r < 1fm$. The *LOCV ASM* NN density distributions at finite temperatures 10, 20 MeV were also computed in the $TSS_z = 110,000$ states. We found that by decreasing the temperature, the probability of finding pairs of nucleons in the 110 and the 000 (the 100 and the 010) states diminishes (enhances). Also, one can study the ratio $R_T \equiv \dfrac{\rho_{010}(r,\theta=\pi/2)}{\rho_{010}(r,\theta=0)}$ to demonstrate the tensor correlation strength in the $T = 0$ states [2]. Due to the similarity of the *LOCV ASM* R_T at finite temperature with that of zero temperature [39], in the present paper, we do not discuss it.

The scaling factor R_{Ad} for the density distributions of light nuclei at short inter-particle distances is proportional to the *Bethe-Levinger* (BL) factor F_{BL}, i.e. $R_{Ad} = F_{BL}\frac{NZ}{A}$ ($N(Z)$ is the number of neutrons (protons)). The ratio of the expectation value of the one-

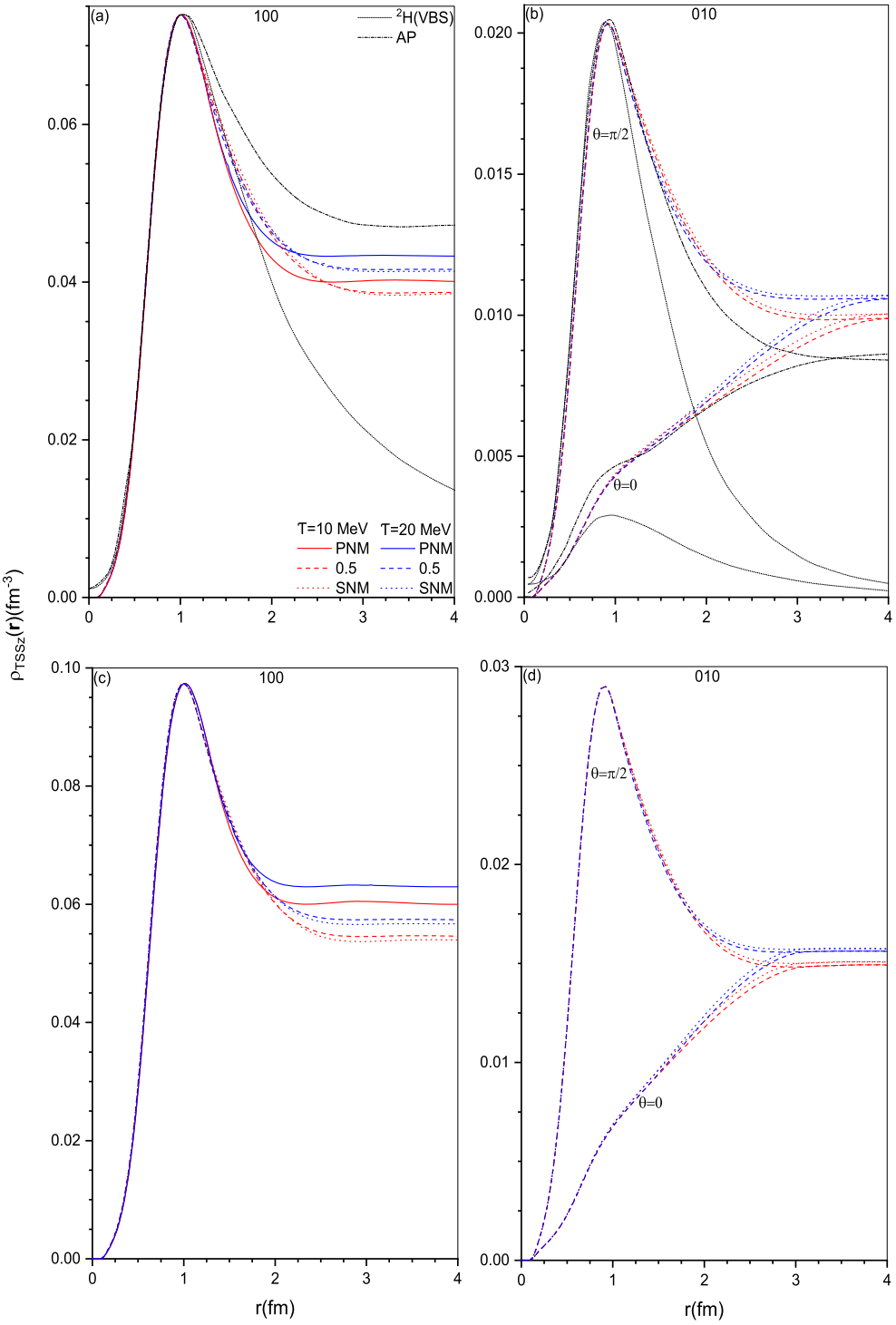

Fig. 3. (a) The *LOCV ASM NN* density distributions, with the $AV18$ [17] interaction and the *TBI* [19], at $\rho = 0.16$ fm^{-3}, in the $TSS_z = 100$ state. The *LOCV ASM* data for $R = 0(PNM), 0.5, 1(SNM)$ at $\mathcal{T}$=10,20 MeV are plotted versus the *VBS* data as well as the *SNM* (AP) calculations of the reference [2]. The *LOCV ASM* $\rho_{100}(\mathbf{r})$ and the corresponding *VBS* and *SNM* data of the reference [2], are scaled to match the maximum value of the *LOCV PNM* $\rho_{100}(\mathbf{r})$ at $\mathcal{T}$=10 MeV. (b) The same as the panel (a) but for the $TSS_z = 010(\theta = 0, \pi/2)$ state. The *LOCV ASM* $\rho_{010}(\mathbf{r})$ and the corresponding ^2H and *SNM* data of the reference [2], are scaled to match the maximum value of the *LOCV SNM* $\rho_{010}(\mathbf{r})$ for $\mathcal{T}$=10 MeV. (c(d)) Similar to the panel (a(b)) but at $\rho = 0.24$ fm^{-3}.

pion exchange part of the $AV18$ interaction of the *ASM* to that of *deuteron*, i.e. $\frac{< V_\Pi >_{ASM}}{< V_\Pi >_d}$, can give us an estimate to the scaling factor R_{Ad} [1]. The scaling factor R_{Ad} predicts the number of *quasideuteron* pairs in the *ASM*. In the panel (a) of the Fig. 4, the ratios $\frac{\frac{1}{A} < V_\Pi >_{ASM}}{< V_\Pi >_d = -21.3 \text{ MeV}}$ for $R = 0.5, 1(SNM)$ at $\mathcal{T}$=0,20 MeV are plotted versus density. The R_{Ad} per nucleon for the *SNM* (*VCS-SNM*) [2] and ^{16}O ($MC-^{16}O$) [1] at $\rho = 0.16$ fm^{-3} and 0.09 fm^{-3} are also given in the mentioned panel for comparison. By increasing the temperature (R and density), the scaling factor (number of *quasideuteron* pairs) per nucleon becomes smaller (larger). At the saturation density $\rho = 0.16$ fm^{-3}, the number of *quasideuteron* pairs per nucleon for $R = 1$ ($R = 0.5$) at $\mathcal{T}$=0,20 MeV are 1.17, 1.07 (1.08, 1.00), respectively. Since the *LOCV* formalism is state-dependent, one should expect that the *LOCV* predictions for the

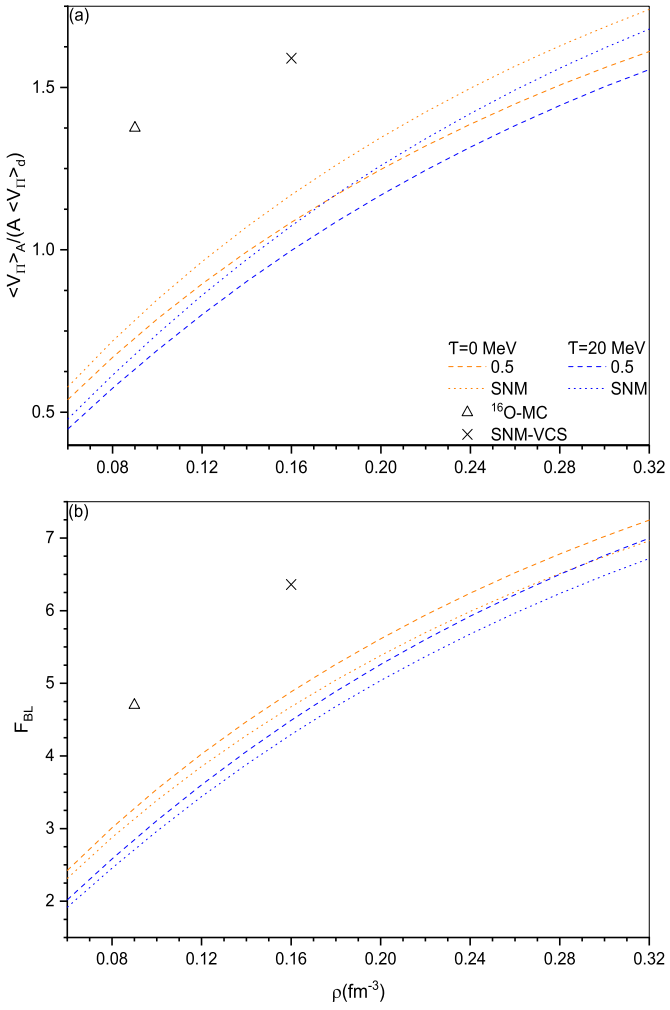

Fig. 4. (a) The ratios $\frac{1}{A} < V_{\Pi} >_{ASM} / < V_{\Pi} >_{d}$ for $R = 0.5, 1(SNM)$ at $\mathcal{T}$=0,20 MeV. The R_{Ad} per nucleon for the *SNM* (*VCS-SNM*) [2] and ^{16}O ($MC-^{16}O$) [1] at $\rho = 0.16$ fm^{-3} and 0.09 fm^{-3} are also given for comparison. (b) The *LOCV ASM* F_{BL} at $\mathcal{T}$=0,20 MeV for $R = 0.5, 1(SNM)$. The F_{BL} for the *SNM* (*VCS-SNM*) [2] and ^{16}O ($MC-^{16}O$) [1] at $\rho = 0.16$ fm^{-3} and 0.09 fm^{-3} are also shown for comparison.

R_{Ad} per nucleon and the F_{BL} lie below those of other many-body techniques.

Considering the scaling factor, we can find the *BL* factor F_{BL}. In the panel (b) of the Fig. 4, the *LOCV ASM BL* factors are shown at $\mathcal{T}$=0 and 20 MeV for $R = 0.5, 1(SNM)$ versus density. The *BL* factor, i.e. $R_{Ad}/4$, for the *SNM* (*VCS-SNM*) [2] and ^{16}O ($MC-^{16}O$) [1] at $\rho = 0.16$ fm^{-3} and 0.09 fm^{-3} are also given in the panel (b) of the Fig. 4. By decreasing the density (temperature and R), the *BL* factor becomes smaller (larger). The *BL* factors at the saturation density $\rho = 0.16$ fm^{-3}, for $R = 1$ ($R = 0.5$) and $\mathcal{T}$=0,20 MeV, are 4.7, 4.3 (4.9, 4.5), respectively. As it is demonstrated in the panel (b) of Fig. 4, the approximated *LOCV SNM* F_{BL} at zero temperature is smaller than those of *VCS* [2] and *MC* [1].

In conclusion, an estimate for the scaling factor (number of *quasideuteron* pairs) was given in the *LOCV* approximation with the use of the two-body $AV18$ potential [17] and the *TBI* of the reference [19]. The dependence of the mentioned factor on the proton to neutron ratio, density, and temperature were also studied. We discussed that, for a given density, the number of *quasideuterons* increases by decreasing (increasing) the temperature (the proton to neutron ratio). Moreover, the probability of finding a pair of nucleons in the TSS_z states was evaluated. It was demonstrated that, at a definite inter-particle distance, by lowering the temperature (proton to neutron ratio), the *NN* density distribution in the $TSS_z = 010$ state grows (diminishes). The present study of the short-range behavior of the *ASM NN* state-dependent density distributions at finite temperature confirms the expected short-range universality. The (non-)central *NN* distribution functions were also investigated. We found that, by increasing the temperature, the tensor-dependent *NN* distribution function becomes weak.

Declaration of competing interest

The authors declare that they have no known competing financial interests or personal relationships that could have appeared to influence the work reported in this paper.

Acknowledgements

I would like to thank the Isfahan University of Technology for their support.

References

[1] J.L. Forest, V.R. Pandharipande, S.C. Pieper, R.B. Wiringa, R. Schiavilla, A. Arriaga, Phys. Rev. C 54 (1996) 646.
[2] A. Akmal, V.R. Pandharipande, Phys. Rev. C 56 (1997) 2261.
[3] B.S. Pudliner, V.R. Pandharipande, J. Carlson, S.C. Pieper, R.B. Wiringa, Phys. Rev. C 56 (1997) 1720.
[4] S.C. Pieper, R.B. Wiringa, V.R. Pandharipande, Phys. Rev. C 46 (1992) 1741.
[5] A. Mukherjee, Phys. Rev. C 79 (2009) 045811.
[6] H. Feldmeier, et al., Phys. Rev. C 84 (2011) 054003.
[7] J.S. Levinger, Phys. Rev. 84 (1951) 43.
[8] J.S. Levinger, Phys. Lett. B 82 (1979) 181.
[9] O.A.P. Tavarest, M.L. Terranova, J. Phys. G, Nucl. Part. Phys. 18 (1992) 521.
[10] K.Sh. Egiyan, et al., Phys. Rev. C 68 (2003) 014313.
[11] K.S. Egiyan, et al., Phys. Rev. Lett. 96 (2006) 082501.
[12] A. Rios, A. Polls, I. Vidana, Phys. Rev. C 79 (2009) 025802.
[13] A. Rios, A. Polls, W.H. Dickhoff, Phys. Rev. C 89 (2014) 044303.
[14] O. Benhar, et al., Nucl. Phys. A 703 (2002) 70.
[15] O. Benhar, et al., Phys. Rev. C 67 (2003) 014326.
[16] C. Ciofi degli Atti, S. Simula, Phys. Rev. C 53 (1996) 1689.
[17] R.B. Wiringa, V.G.J. Stoks, R. Schiavilla, Phys. Rev. C 51 (1995) 38.
[18] I.E. Lagaris, V.R. Pandharipande, Nucl. Phys. A 359 (1981) 349.
[19] A. Tafrihi, Ann. Phys. 409 (2019) 167928.
[20] F. Iwamoto, M. Yamada, Prog. Theor. Phys. 17 (1957) 543.
[21] J.W. Clark, Prog. Part. Nucl. Phys. 2 (1979) 89.
[22] M.E. Grypeos, E. Mavrommatis, Lett. Nuovo Cimento 5 (1972) 369.
[23] J.C. Owen, R.F. Bishop, J.M. Irvine, Phys. Lett. B 59 (1975) 1.
[24] M. Modarres, J.M. Irvine, J. Phys. G, Nucl. Phys. 5 (1979) 511.
[25] M. Modarres, Europhys. Lett. 3 (1987) 1083.
[26] M. Modarres, J. Phys. G, Nucl. Part. Phys. 23 (1997) 923.
[27] G.H. Bordbar, M. Modarres, J. Phys. G, Nucl. Part. Phys. 23 (1997) 1631.
[28] M. Modarres, G.H. Bordbar, Phys. Rev. C 58 (1998) 2781.
[29] G.H. Bordbar, M. Modarres, Phys. Rev. C 57 (1998) 714.
[30] H.R. Moshfegh, M. Modarres, Nucl. Phys. A 759 (2005) 79.
[31] H.R. Moshfegh, M. Modarres, Nucl. Phys. A 749 (2005) 130c.
[32] H.R. Moshfegh, M. Modarres, Nucl. Phys. A 792 (2007) 201.
[33] M. Modarres, A. Rajabi, H.R. Moshfegh, Nucl. Phys. A 808 (2008) 60.
[34] M. Modarres, M. Pourmirjafari, H.R. Moshfegh, Nucl. Phys. A 819 (2009) 27.
[35] M. Modarres, A. Tafrihi, A. Hatami, Nucl. Phys. A 879 (2012) 1.
[36] M. Modarres, A. Tafrihi, Nucl. Phys. A 916 (2013) 126.
[37] M. Modarres, A. Tafrihi, Nucl. Phys. A 941 (2015) 212.
[38] A. Tafrihi, M. Modarres, Nucl. Phys. A 958 (2017) 25.
[39] A. Tafrihi, Ann. Phys. 392 (2018) 12.
[40] Z. Asadi Aghbolaghi, M. Bigdeli, J. Phys. G, Nucl. Part. Phys. 45 (2018) 065101.
[41] S. Goudarzi, H.R. Moshfegh, Phys. Rev. C 91 (2015) 054320.
[42] H. Bahrdo, A. Tafrihi, Eur. Phys. J. A 56 (2020) 27.
[43] M. Rahmat, M. Modarres, Nucl. Phys. A 997 (2020) 121715.
[44] I.E. Lagaris, V.R. Pandharipande, Nucl. Phys. A 369 (1981) 470.
[45] R.B. Wiringa, V. Fiks, A. Fabrocini, Phys. Rev. C 38 (1988) 1010.
[46] W. Zuo, I. Bombaci, U. Lombardo, Phys. Rev. C 60 (1999) 024605.
[47] S. Fantoni, K.E. Schmidt, Nucl. Phys. A 690 (2001) 456.
[48] J. Carlson, J. Morales, V.R. Pandharipande, D.G. Ravenhall, Phys. Rev. C 68 (2003) 025802.

[49] N. Bassan, S. Fantoni, K.E. Schmidt, Phys. Rev. C 84 (2011) 035807.
[50] A. Lovato, O. Benhar, S. Fantoni, A.Yu. Illarionov, K.E. Schmidt, J. Phys. Conf. Ser. 336 (2011) 012016.
[51] S. Gandolfi, A. Lovato, J. Carlson, Kevin E. Schmidt, Phys. Rev. C 90 (2014) 061306(R).
[52] I. Tews, S. Gandolfi, A. Gezerlis, A. Schwenk, Phys. Rev. C 93 (2016) 024305.
[53] X.L. Shang, et al., Phys. Rev. C 101 (2020) 065801.
[54] Z.H. Li, H.-J. Schulze, Phys. Rev. C 78 (2008) 028801.
[55] B.S. Pudliner, V.R. Pandharipande, J. Carlson, R.B. Wiringa, Phys. Rev. Lett. 74 (1995) 4396.